Structural Engineering and Mechanics, *Vol. 68, No. 1 (2018) 39-51*
DOI: https://doi.org/10.12989/sem.2018.68.1.039

A structural model updating method using incomplete power spectral density function and modal data

Akbar Esfandiari*[1], Maryam Ghareh Chaei[2a] and Fayaz R. Rofooei[1a]

[1]Department of Civil Engineering, Sharif University of Technology, Tehran, Iran
[2]Department of Marine Technology, Amirkabir University of Technology, Tehran, Iran

(Received December 26, 2017, Revised July 10, 2018, Accepted July 12, 2018)

Abstract. In this study, a frequency domain model updating method is presented using power spectral density (PSD) data. It uses the sensitivity of PSD function with respect to the unknown structural parameters through a decomposed form of transfer function. The stiffness parameters are captured with high accuracy through solving the sensitivity equations utilizing the least square approach. Using numerically noise polluted data, the model updating results of a truss model prove robustness of the method against measurement and mass modelling errors. Results prove the capabilities of the method for parameter estimation using highly noise polluted data of low ranges of excitation frequency.

Keywords: power spectral density; model updating; frequency response function; sensitivity-based model updating; modal data

1. Introduction

Fatality and money losses due to an abrupt structural failure and also getting the best performance of a structure during its lifetime are important goals which are considered while designing structures. These motivations caused civil, mechanical and aerospace engineers to seek approaches for detecting the presence and location of structural damage as well as damage severity. Current non-destructive experimental methods such as acoustic or ultrasonic methods, magnetic field methods, eddy current methods or thermal field methods require the vicinity of the damaged parts to be known and accessible. In order to remove these drawbacks some techniques are proposed which use structural responses of the damaged structure to identify the damage location and severity (Doebling *et al.* 1998 , Fan and Qiao 2011). Based on the structural responses used for damage detection, these methods are categorized into two main groups, static based and vibration based structural model updating methods. In the static response based methods, measurement of displacement or strain are the basis of damage detection algorithms. However, the underlying idea of vibration-based damage identification methods is the contingency of the dynamic characteristics and structural responses to their physical properties such as mass, stiffness and damping, which are affected by structural damages. Therefore, one may extract the location and intensity of the structural damages from vibration data of the damaged structure. Vibration-based damage identification methods can be categorized by the dynamic characteristic data that are used, or by the employ approach to correlate the dynamic properties and structural damages. Some techniques investigate changes in natural frequencies (Wang and Li 2012, Min *et al.* 2014), mode shapes (Xu and Zhu 2017, Yazdanpanah *et al.* 2015), curvature of modes (Ditommaso *et al.* 2015), modal strain energy (Entezami *et al.* 2017) or dynamic flexibility (Wei *et al.* 2016, Zhang *et al.* 2013) to locate and quantify damage in a structure. There are other methods toward this purpose using frequency response functions (FRF) (Gang *et al.* 2014, Beyhaqi and Esfandiari 2017) and power spectral density function (Pedram *et al.* 2017, Eun *et al.* 2015, Liberatore *et al.* 2001). Environmental phenomena, not stationary and/or nonlinear behaviour of the structures affect dynamic responses and cause to variation of the characteristics indices such as natural frequencies (Ditommaso *et al.* 2012 and Petrovic *et al.* 2017). Extraction of the dynamic characteristic of the structure and distinguishing these variations are studied by many researchers (Ditommaso and Ponzo 2015).

Model updating damage detecting methods can be categorized as iterative and non-iterative algorithms. The non-iterative methods require measurements in all DOFs of the damaged structure which is not practical. Also, the changes which are the basis of damage detection in this category are changes in global structural matrix so that they do not have physical interpretation. On the other hand, the iterative approaches are used successfully based on the incomplete measured data, while the change of unknown parameters can be interpreted physically. Iterative model updating methods can be conducted by sensitivity-based,

*Corresponding author, Ph.D.
E-mail: A_Esfandiari@aut.ac.ir
[a]M.Sc. Student
E-mail: maryamgharechaei@yahoo.com
[b]Professor
E-mail: rofooei@sharif.edu

http://www.techno-press.com/journals/sem&subpage=7
ISSN: 1225-4568 (Print), 1598-6217 (Online)

genetic algorithms and neural network approaches. The two latter methods use random search. So, they have less convergence rate and more computation expense.

Model updating methods can be categorized into the model based and non-model based methods or it can also be categorized into the direct or iterative methods. The exact analytical model of both damaged and intact structures are needed in the model based methods, whereas only the damaged structure model is needed in the latter. Non-model based methods cannot successfully perform with incomplete measurements and mostly fail to identify the severity of the damage.

Based on the data used for structural model updating, some methods are formulated in the frequency-domain, while the others are casted in time-domain (Natke *et al.* 1995). Frequency domain approaches have drawn more attention due to less data volume and more sensitive damage indices in comparison to the time domain approaches. Dos Santos *et al.* (2005) proposed a damage detection method based on frequency response functions (FRF) sensitivities. Their technique leads to a set of sensitivity equations, which are solved using an algorithm that constrains the solution to be physically admissible. They performed a damage simulation and identification on a laminated rectangular plate. Esfandiari *et al.* (2009) correlated the changes of the measured FRF data to the changes of stiffness, mass and damping properties through damage sensitivity equations, which are solved using the least square method. Based on the decomposed form of the transfer function and measured natural frequencies of the damaged structure, an approximated expression is used to deal with the incomplete measurement challenges. Esfandiari et al (2010) expressed a sensitivity relation for the decomposed FRF based on the sensitivity of the mode shapes.

Although FRF based methods have drawn a lot of attention, power spectral density function provides the possibility to considering the statistic and random characteristics of the structural response and incorporating the random inputs into damage detection approaches. Moreover, since the cross spectral terms are considered in PSD-based methods, more data are provided comparing to using only auto spectral terms. Furthermore, PSD is a second order function of the FRF and exgabits more sensitive behaviour with respect to the structural parameters. Kammer and Nimityongskul (2009) expressed several advantages of using PSD over FRF, such as the ability to easily include data from all inputs at once and the real metric. Thus, the PSD based damage detection methods are intended to be more accurate than FRF-based ones. Kumar *et al.* (2012) identified the structural damages in a lightly reinforced concrete beam based on changes in the PSD data. Liberatore and Carman (2004) proposed a method for identification and localization of the structural damages using the most sensitive frequency ranges which are the narrow frequency band widths around the near resonance. They estimated the corresponding energy by power spectral density analysis and calculated the average and root mean square values. These values were used along with the mode shapes data to locate structural damages of an experimental beam. The method does not allocate the severity of the damage.

Zheng *et al.* (2015) proposed a new model updating method based on the power spectral density sensitivity analysis. They used the pseudo excitation method to calculate structural responses and PSD under stationary and random excitations. Li *et al.* (2015a, b) used experimental data of a steel frame for damage identification based on the power spectral density transmissibility (PSDT). The sensitivity relation is calculated numerically by the finite difference method. The location and severity of the introduced structural damages are detected accurately. Pedram *et al.* (2016) proposed the exact relation of the changes of the PSD with respect to structural parameters. An approximated evaluation is used to estimate unmeasured parts of structural responses. Pedram *et al.* (2017) updated the FE model of a laboratory concrete beam for identification of extensive distributed damage cases using PSD data.

This study focuses on proposing a structural damage detection method based on the power spectral density data and a subset of the measured natural frequencies of the damaged structure. Structural damage is considered as the reduction in structural stiffness parameters. The sensitivity equations are formulated implicitly through expressing the change of the power spectral density function in terms of the changes of structural parameters. The proposed method minimized a defined residual by using PSD data of the damage structure and an evaluated value using the incomplete measured modal data. The sensitivity relation of the power spectral density function is derived using the decomposed form of the transfer function and the changes of the mode shapes. The least square method is adopted to solve the sensitivity equation set through a proper weighting procedure. The results prove that the proposed method is capable of detecting and localizing structural damages and is robust against measurement and mass modeling errors.

2. Theory

The power spectral density function of a system can be defined as (Newland 1993)

$$\mathrm{S_{xx}}(\omega) = \mathrm{H}(\omega)\mathrm{S_{ff}}(\omega)\mathrm{H}^*(\omega)^T \tag{1}$$

Where $\mathrm{H}(\omega)$, $\mathrm{S_{xx}}(\omega)$ and $\mathrm{S_{ff}}(\omega)$ are the frequency response function, power spectral density of response and applied force respectively. $\mathrm{H}^*(\omega)$ is the complex conjugate of the transfer function. The frequency response function of a system with n degrees of freedom is defined as

$$\mathrm{H}(\omega) = [-\mathrm{M}\omega^2 + \mathrm{i}\omega\mathrm{C} + \mathrm{K}]^{-1} \tag{2}$$

Where M, C and K are mass, damping and stiffness matrices of the structure, respectively, and ω is the frequency of the excitation load. The power spectral density function of the damaged structure can be defined as

$$\mathrm{S_{xxd}}(\omega) = \mathrm{H_d}(\omega)\mathrm{S_{ff}}(\omega)\mathrm{H^*}_{\mathrm{d}}(\omega)^{\mathrm{T}} \tag{3}$$

Where $\mathrm{H_d}(\omega)$ and $\mathrm{S_{xxd}}(\omega)$ are the frequency response function and the response power spectral density of the damaged system, respectively. In order to establish a relation between the spectral density of the damaged structure and the changes of structural parameters, the decomposed form of H_d is used as (Esfandiari *et al.* 2010)

$$H_{il}(\omega) = \sum_{r=1}^{n} \frac{\Phi_{ir}\,\Phi_{lr}}{\omega_r^2 - \omega^2 + 2i\omega\xi_r\omega_r} \tag{4}$$

$H_{il}(\omega)$ represents the FRF of the structure at the *ith* degree of freedom subjected to the excitation load at the *lth* degree of freedom. Φ_r, ω_r and ξ_r represent the *rth* mode shape, natural frequency and damping ratio, respectively. Considering Eq. (3), the frequency response function of the damaged structure should be calculated. The *rth* mode shape of the structure after changes due to the damage is expressed as

$$\Phi_{rd} = \Phi_r + \delta\Phi_r \tag{5}$$

Where the index "d" ndicates to the damaged structure and $\delta\Phi_r$ represents the changes in the *rth* mode shape due to the damage. Substituting Eq. (5) in Eq. (4) for the damaged structure leads to

$$H_{ild}(\omega) = \sum_{r=1}^{n} \frac{(\Phi_{ir} + \delta\Phi_{ird})(\Phi_{lr} + \delta\Phi_{lrd})}{\omega_{rd}^2 - \omega^2 + 2i\omega\xi_{rd}\omega_{rd}} \tag{6}$$

Supposing that the first nm natural frequencies of the damaged structure are measurable and neglecting the second order term, Eq. (6) can be rewritten as

$$H_{ild}(\omega) \cong \sum_{r=1}^{nm} \frac{\Phi_{ir}\Phi_{lr}}{\omega_{rd}^2 - \omega^2 + 2i\omega\xi_{rd}\omega_{rd}} + \sum_{r=1}^{nm} \frac{\Phi_{ir}\delta\Phi_{lr}}{\omega_{rd}^2 - \omega^2 + 2i\omega\xi_{rd}\omega_{rd}} \tag{7}$$

As the measurement of the natural frequencies is feasible with high accuracy, the evaluated value by Eq. (7) is realistic. The first term of this equation can be calculated using the properties of the intact structure and measured natural frequencies of the damaged structure. The last term of the Eq. (7) is added to the formulation to approximate the unmeasured parts of the modal data related to the higher mode shapes and compensates the effect of incomplete measurement. Moreover, the other terms (the second and third terms) of the equation include the mode shape changes, should be evaluated as function of structural parameters. Accurate formulation of the mode shape changes yield to the reliable parameter estimation results. By separating the known and unknown terms of Eq. (7), it can be rewritten as

$$H_{ild}(\omega) \cong \widetilde{H}_{il}(\omega) + \Delta\overline{H}_{il}(\omega) \tag{8}$$

Where

$$\widetilde{H}_{il}(\omega) = \sum_{r=1}^{nm} \frac{\Phi_{ir}\Phi_{lr}}{\omega_{rd}^2 - \omega^2 + 2i\omega\xi_{rd}\omega_{rd}} + \sum_{r=nm+1}^{n} \frac{\Phi_{ir}\Phi_{lr}}{\omega_r^2 - \omega^2 + 2i\omega\xi_r\omega_r} \tag{9}$$

And

$$\Delta\overline{H}_{il}(\omega) = \sum_{r=1}^{nm} \frac{\Phi_{ir}\delta\Phi_{lr}}{\omega_{rd}^2 - \omega^2 + 2i\omega\xi_{rd}\omega_{rd}} + \sum_{r=1}^{nm} \frac{\delta\Phi_{ir}\Phi_{lr}}{\omega_{rd}^2 - \omega^2 + 2i\omega\xi_{rd}\omega_{rd}} \tag{10}$$

To estimate $\Delta\overline{H}_{il}(\omega)$ which contains the unknown terms of Eq. (7), the rate of changes of mode shapes is considered as a linear combination of the eigenvectors of the analytical model. Thus, the mode shape changes can be defined by the following expression (Fox and Kapoor 1969)

$$\delta\Phi_r \cong \sum_{q=1}^{n} \alpha_{rq}\Phi_q \tag{11}$$

Where

$$\begin{cases} \alpha_{rq} = \dfrac{{\Phi_q}^T(\delta K - {\omega^2}_i\delta M)\Phi_i}{\left({\omega_r}^2 - {\omega_q}^2\right)} & \text{for } q \neq r \\ \alpha_{rr} = -\dfrac{{\Phi_r}^T(\delta M)\Phi_r}{2} & \text{for } q = r \end{cases} \tag{12}$$

α_{rq} is the participation factor of the qth mode shapes for evaluation of the changes of the *rth* mode shape. For most structures, the mass changes are negligible in reality. Therefore, only the stiffness properties are considered as the unknown parameters of the model updating process. In that case, α_{rq} is equal to

$$\alpha_{rq} = \frac{{\Phi_q}^T(\delta K)\Phi_i}{\left({\omega_r}^2 - {\omega_q}^2\right)} \tag{13}$$

Substituting Eq. (13) in Eq. (10), it can be rewritten as

$$\Delta\overline{H}_{il}(\omega) = \sum_{r=1}^{nm}\sum_{q=1}^{n} \frac{\Phi_{ir}({\Phi_q}^T\delta K\Phi_r)\Phi_{lq}}{(\omega_{rd}^2 - \omega^2 + 2i\omega\xi_{rd}\omega_{rd})\left({\omega_r}^2 - {\omega_q}^2\right)} + \sum_{r=1}^{nm}\sum_{q=1}^{n} \frac{\Phi_{lr}({\Phi_q}^T\delta K\Phi_r)\Phi_{iq}}{(\omega_{rd}^2 - \omega^2 + 2i\omega\xi_{rd}\omega_{rd})\left({\omega_r}^2 - {\omega_q}^2\right)} \tag{14}$$

The stiffness matrix of each element of a structure can be defined as

$$K_e = A_e P_e {A_e}^T \tag{15}$$

Where A_e is the eigenvector of nonzero eigenvalues of the stiffness matrix which shows the geometrical properties of the elements and P_e is the corresponding nonzero eigenvalue of the stiffness matrix which contains mechanical properties.

By assembling the stiffness matrices of all elements, the stiffness matrix of the structure in the global coordinates is defined as

$$K = \sum_{i-1}^{ne} T_{ei}^T A_{ei}\, P_{ei} A_{ei}^T T_{ei} = APA^T \tag{16}$$

Where T_{ei} is the transformation matrix of the *ith* element from the local to global coordinate and ne is the total number of elements. The stiffness matrix of the damaged structure can be defined as

$$\mathrm{K_d} = \mathrm{K} + \delta\mathrm{K} = \mathrm{A}(\mathrm{P} + \delta\mathrm{P})\mathrm{A}^{\mathrm{T}} \tag{17}$$

Where $\delta\mathrm{P}$ is the change of elemental stiffness due to damage. Subtracting Eq. (16) from Eq. (17), $\delta\mathrm{K}$ can be expressed as

$$\delta\mathrm{K} = \mathrm{A}\delta\mathrm{P}\mathrm{A}^{\mathrm{T}} \tag{18}$$

Substituting Eq. (18) in Eq. (14) leads to

$$\begin{aligned} &\Delta\overline{\mathrm{H}}_{\mathrm{il}}(\omega) \\ &= \left[\sum_{r=1}^{nm}\sum_{q=1}^{n}\frac{\Phi_{\mathrm{ir}}(\Phi_{\mathrm{q}}{}^{\mathrm{T}}\mathrm{Adiag}(\mathrm{A}^{\mathrm{T}}\Phi_{\mathrm{r}}))\Phi_{\mathrm{lq}}}{(\omega_{\mathrm{rd}}^2-\omega^2+2\mathrm{i}\omega\xi_{\mathrm{rd}}\omega_{\mathrm{rd}})(\omega_{\mathrm{i}}{}^2-\omega_{\mathrm{q}}{}^2)}\right. \\ &\left.+\sum_{r=1}^{nm}\sum_{q=1}^{n}\frac{\Phi_{\mathrm{iq}}(\Phi_{\mathrm{q}}{}^{\mathrm{T}}\mathrm{Adiag}(\mathrm{A}^{\mathrm{T}}\Phi_{\mathrm{r}}))\Phi_{\mathrm{lr}}}{(\omega_{\mathrm{rd}}^2-\omega^2+2\mathrm{i}\omega\xi_{\mathrm{rd}}\omega_{\mathrm{rd}})(\omega_{\mathrm{i}}{}^2-\omega_{\mathrm{q}}{}^2)}\right]\delta\mathrm{P} \end{aligned} \tag{19}$$

Where, the operator $diag$ converts a vector to a diagonal matrix and vice versa. By naming the coefficient of $\delta\mathrm{P}$ as $\mathrm{S_H}$, and considering Eq. (19), Eq. (8) can be rewritten as

$$\mathrm{H_{ild}}(\omega) \cong \widetilde{\mathrm{H}}_{\mathrm{il}}(\omega) + \mathrm{S}_H^{(i,l)}(\omega)\delta\mathrm{P} \tag{20}$$

The matrices $\mathrm{S_H}$ express the $\Delta\overline{\mathrm{H}}_{\mathrm{il}}(\omega)$ as a function of the unknown parameters. The (k,j) entries of the power spectral density function of the damaged structure can be expressed as

$$\begin{aligned} \mathrm{S}_{\mathrm{xxd}}^{(k,j)}(\omega) &\cong \widetilde{\mathrm{H}}_k(\omega)\mathrm{S_{ff}}(\omega)\widetilde{\mathrm{H}}_j^*(\omega)^{\mathrm{T}} \\ &+ \Delta\overline{H}_k(\omega)\mathrm{S_{ff}}(\omega)\widetilde{\mathrm{H}}_j^*(\omega)^{\mathrm{T}} \\ &+ \widetilde{\mathrm{H}}_k(\omega)\mathrm{S_{ff}}(\omega)\Delta\overline{H}_j^*(\omega)^{\mathrm{T}} \\ &+ \Delta\overline{H}_k(\omega)\mathrm{S_{ff}}(\omega)\Delta\overline{H}_j^*(\omega)^{\mathrm{T}} \end{aligned} \tag{21}$$

$\widetilde{\mathrm{H}}_k(\omega)$ and $\widetilde{\mathrm{H}}_j(\omega)$ represents the kth and jth rows of the $\widetilde{\mathrm{H}}(\omega)$. By subtracting the first term at the right hand side of Eq. (21) from the left hand side, $\Delta\mathrm{S_{xx}}(\omega)$ can be defined as

$$\begin{aligned} &\Delta\mathrm{S}_{\mathrm{xxd}}^{(k,j)}(\omega) = \mathrm{S}_{\mathrm{xxd}}^{(k,j)}(\omega) - \widetilde{\mathrm{S}}_{\mathrm{xxd}}^{(k,j)}(\omega) \\ &\text{and} \qquad \widetilde{\mathrm{S}}_{\mathrm{xxd}}^{(k,j)}(\omega) = \widetilde{\mathrm{H}}_k(\omega)\mathrm{S_{ff}}(\omega)\widetilde{\mathrm{H}}_j^*(\omega)^{\mathrm{T}} \end{aligned} \tag{22}$$

$\mathrm{S}_{\mathrm{xxd}}^{(k,j)}(\omega)$ is the PSD of the damaged structure and $\widetilde{\mathrm{S}}_{\mathrm{xxd}}^{(k,j)}(\omega)$ is calculated using the properties of the intact structure and the measured natural frequencies and damping ratios of the damaged structure. Hence, $\Delta\mathrm{S}_{\mathrm{xxd}}^{(k,j)}(\omega)$ has a known value.

Using Eq. (20), $\Delta\overline{\mathrm{H}}_{\mathrm{k}}(\omega)$ which represents the $\mathrm{k^{th}}$ row of the matrix $\Delta\overline{\mathrm{H}}(\omega)$ can be expressed as

$$\Delta\widetilde{\mathrm{H}}_k^T(\omega) = \begin{bmatrix} \mathrm{S}_H^{(1,k)}(\omega) \\ \mathrm{S}_H^{(2,k)}(\omega) \\ \vdots \\ \mathrm{S}_H^{(n,k)}(\omega) \end{bmatrix}\delta\mathrm{P} = \mathrm{S}_H^k(\omega)\delta\mathrm{P} \tag{23}$$

Using Eq. (23) and neglecting the second order term, Eq. (21) can be rewritten as

$$\begin{aligned} \Delta\mathrm{S}_{\mathrm{xxd}}^{(k,j)}(\omega) &\cong \Delta\overline{\mathrm{H}}_{\mathrm{k}}(\omega)\mathrm{S_{ff}}(\omega)\widetilde{\mathrm{H}}_j^*(\omega)^{\mathrm{T}} \\ &+ \widetilde{\mathrm{H}}_k(\omega)\mathrm{S_{ff}}(\omega)\Delta\overline{\mathrm{H}}_j^*(\omega)^{\mathrm{T}} \\ &= S_{PSD}^{(k,j)}(\omega)\delta\mathrm{P} \end{aligned} \tag{24}$$

Where

$$\begin{aligned} S_{PSD}^{(k,j)}(\omega) &= \widetilde{\mathrm{H}}_j^*(\omega)\mathrm{S_{ff}}(\omega)\mathrm{S}_H^k(\omega) \\ &+ \widetilde{\mathrm{H}}_k(\omega)\mathrm{S_{ff}}(\omega)\mathrm{S}_H^j(-\omega)^{\mathrm{T}} \end{aligned} \tag{25}$$

For all measured responses, cross spectral density and auto spectral density values can be represented as

$$\Delta\mathrm{S_{xx}}(\omega) = \mathrm{S}_{PSD}(\omega)\ \delta\mathrm{P} \tag{26}$$

Where $\mathrm{S}_{PSD}(\omega)$ is the sensitivity matrix and $\delta\mathrm{P}$ is the vector of stiffness parameter changes. It is possible to solve Eq. (26) with different methods such as the least square method (LS), non-negative least square (NNLS) and singular value decomposition method (SVD). In this study the least square method is used to solve the equation.

Equations with larger coefficients may dominate the least square solution. Therefore, a weighting technique should be used to prevent overshadowing the information of some equations by some others. There are different methods for weighting the equations. The sensitivity of the PSD increases at higher frequency ranges. However, due to large approximations of the formulation of the changes of the mode shapes at higher frequencies (higher mode shapes), the weight of the sensitivity equations in this range must be decreased. Thus, in this study each sensitivity equation is multiplied by $\omega^{-0.5}$.

Another noteworthy issue in sensitivity-based model updating methods is the noise polluted the experimental data which may cause a convergence to a local minimum. In the vicinity of natural the frequencies of the damaged structure this noise can have serious effects on the response because of the term $\omega_{\mathrm{d}}^2 - \omega^2$ in the derived equations. There are other sources of errors which can cause problems in such methods like mass modeling errors which means the error associated with the mass of modeled intact structures and the errors of measuring natural frequencies. Therefore, the proposed methods in this field should be robust to these errors and noises.

3. Numerical simulation

A 2-D truss is modeled using the finite element model of the structure consisting of 35 elements and 16 DOFs which is shown in Fig. 1. The elements are made of steel with Young's modulus of 200 Gpa. Cross sectional area of elements are given in Table 1. The kinematic DOFs of the truss model are shown in Fig. 2.

Measurement and excitation setup; Selection of the excitation and measurement locations is a challenging issue for successful structural model updating (Bruggi and Mariani 2013, Sanayei and Onipede 1991). At the selected excitation and measurement locations, all structural

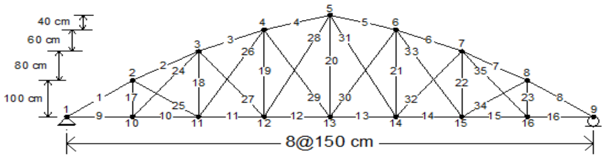

Fig. 1 Geometry of the truss model

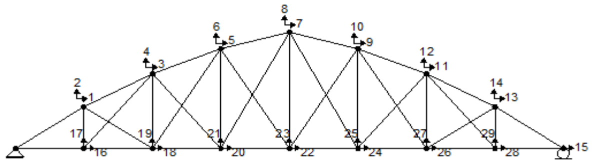

Fig. 2 Active degrees of freedom of the truss model

Table 1 Cross sectional area of the truss elements

Element Number	Area Cm^2
1-8	18
9-16	15
17-23	10
24-35	12

Table 2 Various groups of excitation and measurement DOFs

1st group	Measurement DOFs	2-5-11-20-22
	Excitation DOFs	1-3-8-15-21-26-29
2nd group	Measurement DOFs	9-13-15-17-19
	Excitation DOFs	7-9-11-14-17-18-27-28
3rd group	Measurement DOFs	1-3-12-19-25
	Excitation DOFs	4-7-10-23-26-29
4th group	Measurement DOFs	6-7-12-19-21
	Excitation DOFs	3-7-12-21-24-28

elements must contribute to structural response and exhibit enough contribution to sensitivity matrix to guaranty their observability. In order to find the proper places for installing the sensors and measuring equipment, several groups of DOFs are considered as the measurement and excitation locations. The selected groups of excitation and measurement DOFs are shown in Table 2.

All selected groups of DOFs are used to identify structural parameters of the intact structure (damage is considered to be zero) using noise polluted data. It is assumed that the structure is excited at the selected DOFs individually and structural responses are measured at the corresponding DOFs. After running the program, for each selected group of DOFs, the one which exhibit best performance in identifying the properties of the structure is considered to be the excitation and measuring DOFs. Here, among the selected groups, the 2nd group led to more accurate results. Therefore, the excitation loads are applied at the DOF numbers 9, 13, 15, 17 and 19 individually. Hence, the corresponding diagonal entity of the matrix $S_{ff}(\omega)$ is set as 1 for each excitation load. The rest of the entities of $S_{ff}(\omega)$ matrix remain zero. Also, DOF numbers

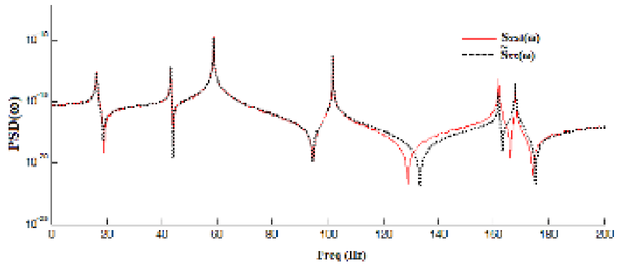

Fig. 3 Calculated $\tilde{\mathbf{S}}_{\mathbf{xxd}}(\boldsymbol{\omega})$ using the intact structure properties and measured modal data Vs. Measured PSD

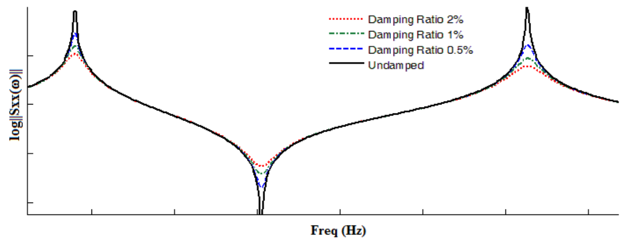

Fig. 4 A template of the calculated $S_{xx}(\omega)$ for damped and undamped structure

7, 9, 11, 14, 17, 18, 27 and 28 are chosen as measurement location. The excitation and measurement locations are same for all damage cases.

The location, severity and number of the defected elements can affect the results of the parameter estimation process. Therefore, several damage scenarios are considered to investigate the abilities of the proposed parameter estimation method. Details of the damage cases are shown as bar charts in the related figures. In practical cases, the power spectral density data of the damaged structure should be available from an experimental setup. Here, the finite element method is adopted to simulate the PSD data damaged structure. It is assumed that the power spectral density of a limited number of DOFs and the first ten natural frequencies of the damaged structure are available for the FE model updating process. Some simulated measurement errors are considered in regard to probable experimental errors, i.e. mass modeling errors, natural frequency and PSD measurement errors. The application of these errors is explained later.

Excitation frequencies; For a sensitivity based model updating method selection of the proper ranges of the excitation frequencies is a challenging issue. At the selected excitation frequencies, the residuals at the left hand side of the sensitivity equation must be large enough for a successful model updating against measurement errors. This method attempts to minimize the residual which is obtained by subtraction of the PSD of the damaged structure $S_{xxd}(\omega)$, and the estimated value of $\tilde{S}_{xxd}(\omega)$. A template of these functions is shown in Fig. 3.

As this figure shows, differences between $S_{xxd}(\omega)$ and $\tilde{S}_{xxd}(\omega)$ are large at the higher frequencies generally. Therefore, model updating must be conducted at these frequency ranges. The selected ranges are near resonance but they do not include the resonance frequencies.

Damping modeling; By the proposed method the

Table 3 Selected frequency ranges for structural model updating

Damage Scenario	1	2	3	4	5	6
Frequency Range	218-224	218-223	221-226	222-227	209-214	250-255
	228-234	227-232	230-235	231-236	218-223	259-264
	288-294	301-306	294-299	292-297	293-298	303-308
	298-305	310-315	303-308	302-304	302-307	312-317
	313-319	319-324	314-319	308-313	313-318	332-337
	323-330	328-333	323-328	329-334	322-327	341-346

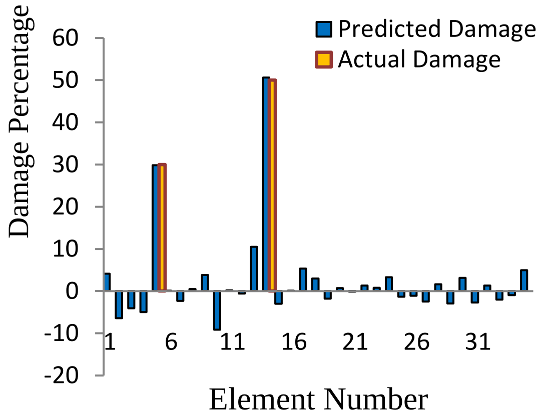

Fig. 5 The actual and predicted damage for the first damage scenarios using noisy data

damped power spectral density could be used for FE model updating. However, measurement of the modal damping ratios is challenging issue and is not as accurate as natural frequencies measurement. Furthermore, damping models might not be able to represent the structural responses as accurate as needed in FE model updating. Any shortcoming of damping models affects the model updating results as a modeling error issue. A temple of PSD for different damping ratios is presented by Fig. 4.

As this figure shows, damping phenomena influences the power spectral density in narrow frequency zones which are so close to resonance frequencies. Therefore, in this study model updating is conducted at the excitation frequencies away from these zones. At these frequency ranges, structural responses are not dominated by damping and element level updating of damping parameters is ignored. It is noted that damping parameter updating at the element level might not be meaningful. In most cases, damping is due to nonstructural elements, energy radiation from foundation, and structural connection details which are not included directly in most structural models. Despite of large amplitude of the PSD at these frequency ranges and accurate response measurement, numerical simulation for parameter estimation prove deviation of the results by considering damping modeling errors. The selected frequency ranges for structural model updating are summarized in Table 3.

As mentioned before, in this study the natural frequencies and the PSD data are simulated numerically. In practical cases, there are some errors in the measurement

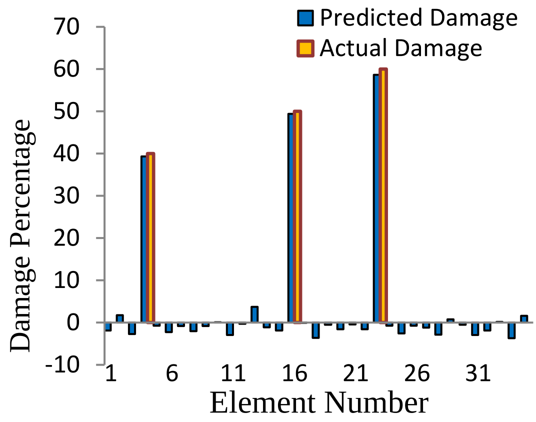

Fig. 6 The actual and predicted damage for the second damage scenarios using noisy data

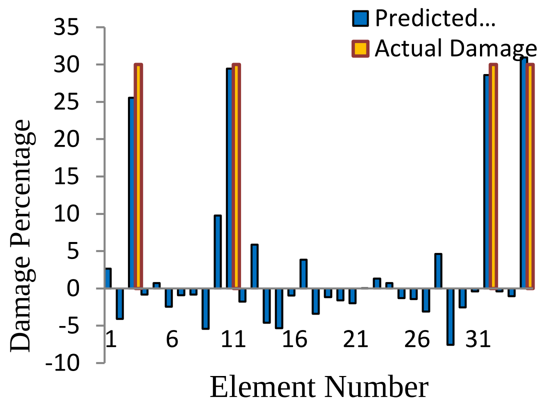

Fig. 7 The actual and predicted damage for the third damage scenarios using noisy data

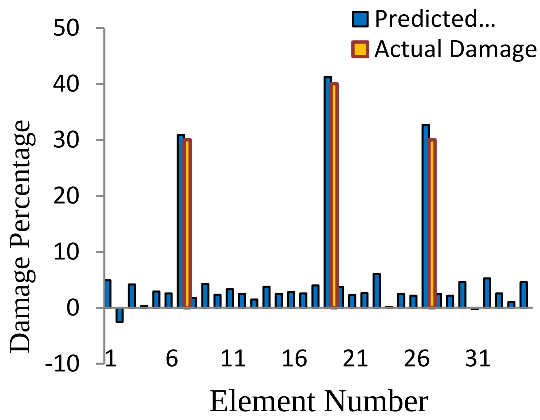

Fig. 8 The actual and predicted damage for the fourth damage scenarios using noisy data

and data processing that adversely affects the results. Here, 10% of uniformly distributed random errors are included in the PSD data computed by the FE method to involve the measurement errors. 100 set of the noise polluted data are used for the parameter estimation process. The averages of the predicted parameters are presented as the model updating results in Figs. 5 to 10.

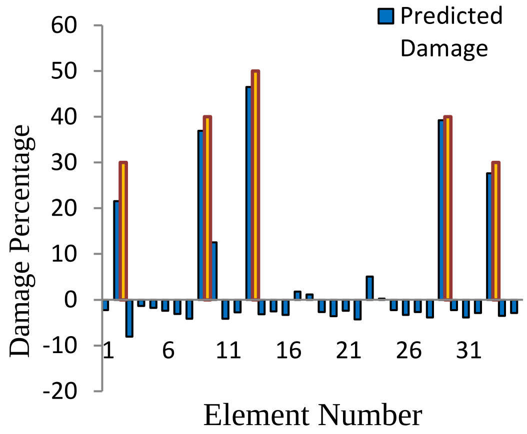

Fig. 9 The actual and predicted damage for the fifth damage scenarios using noisy data

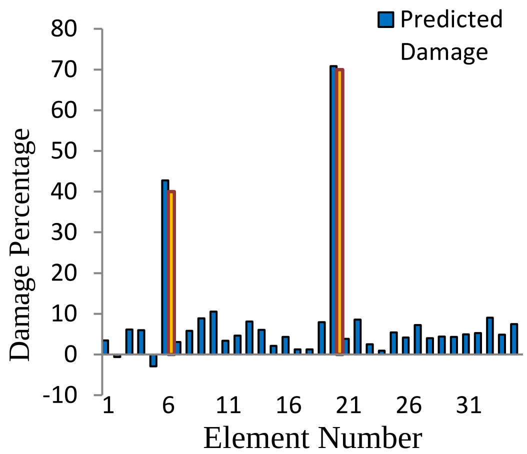

Fig. 10 The actual and predicted damage for the sixth damage scenarios using noisy data

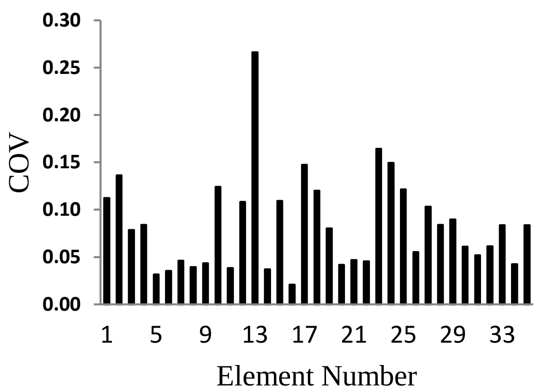

Fig. 11 COVs of estimated parameters of the first damage scenarios

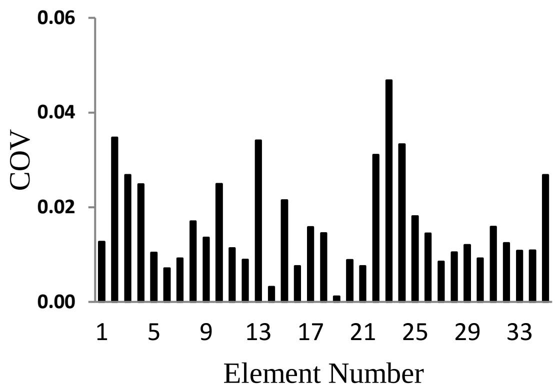

Fig. 12 COVs of estimated parameters of the second damage scenarios

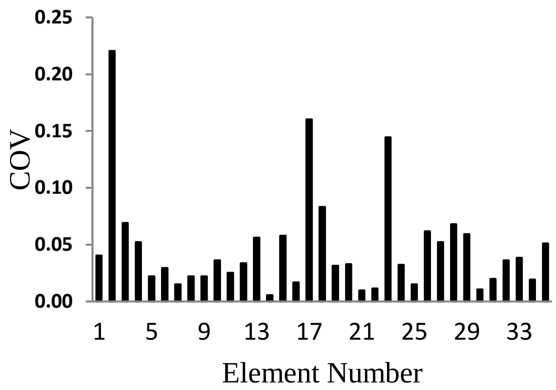

Fig. 13 COVs of estimated parameters of the third damage scenarios

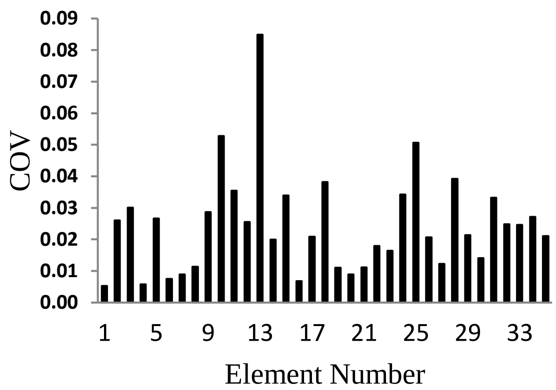

Fig. 14 COVs of estimated parameters of the forth damage scenarios

The results indicate that the performance of the proposed approach for structural damage identification is promising. In order to investigate the scattering of the estimated parameters around averages, coefficient of variations (COV) of the predicted unknown parameters (standard deviation divided by the mean value) are also presented in Figs. 11 to 16.

Small values of COVs indicate that the results are less scattered around averages and show the robustness of the method against measurement errors.

Existing advanced sensors makes the measurement of natural frequencies very accurate, such that some

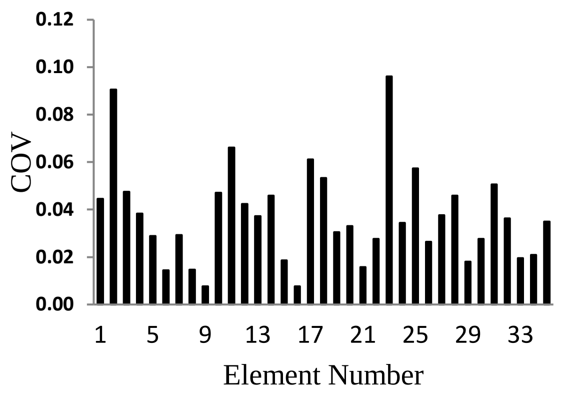

Fig. 15 COVs of estimated parameters of the fifth damage scenarios

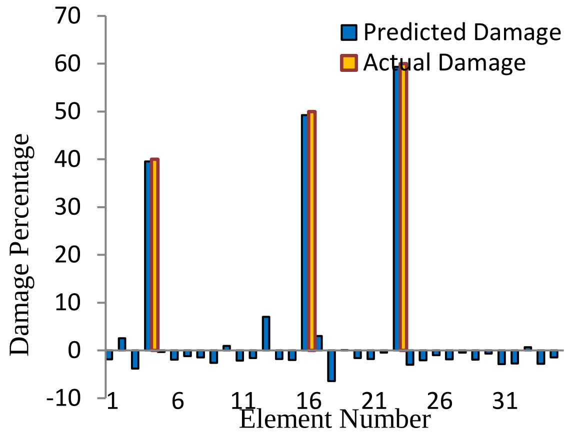

Fig. 17(a) The actual and predicted damage for the second damage scenarios considering 0.5% natural frequencies error

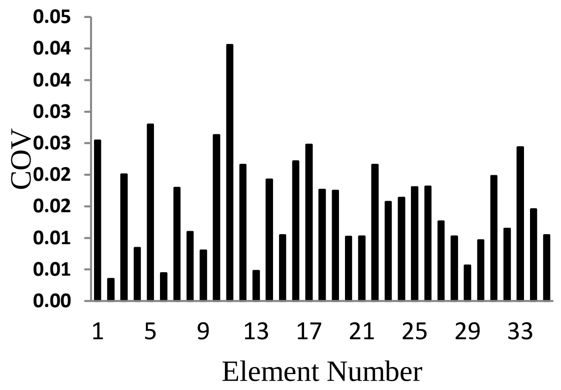

Fig. 16 COVs of estimated parameters of the sixth damage scenarios

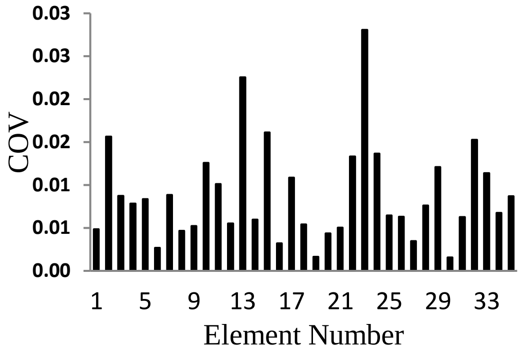

Fig. 17(b) COVs of estimated parameters for second damage scenarios considering 0.5% natural frequencies error

researchers assume it as a noise-free measurement of resonances. If the excitation frequency for model updating is not in the vicinity of the nearest measured resonances any unexpected errors in natural frequencies does not affect the results of parameter estimation. For a lightly damped structure, the denominators of Eq.(7), and consequently the sensitivity matrix are dominated by $\omega_{id}^2 - \omega^2$. If the excitation frequency is selected close to the resonance frequency small errors in the measured resonances introduce a significant change in the value of $\omega_{id}^2 - \omega^2$, causing large deviation in the sensitivity equations. The adverse effects of this type of error can be reduced by moving away from the resonance frequency. In order to investigate the effects of noise polluted natural frequencies on model updating results, 0.5% of uniformly distributed random errors are introduced in the natural frequencies of the damaged structure. Two template of the model updating results and their COVs are shown in Figs. 17 and 18. As, these figures indicate, the proposed model updating algorithm is capable of the parameter estimation in the presence of errors in the measured natural frequencies. Small COVs of the predicted stiffness parameters indicate robustness of the method against this type of measurement

Table 4 CI indices of the model updating results considering 0.5% natural frequencies errors

Damage Scenarios		CI
2	0.5% natural frequencies errors	0.92
	Noise free frequency	0.97
6	0.5% natural frequencies errors	0.90
	Noise free frequency	0.94

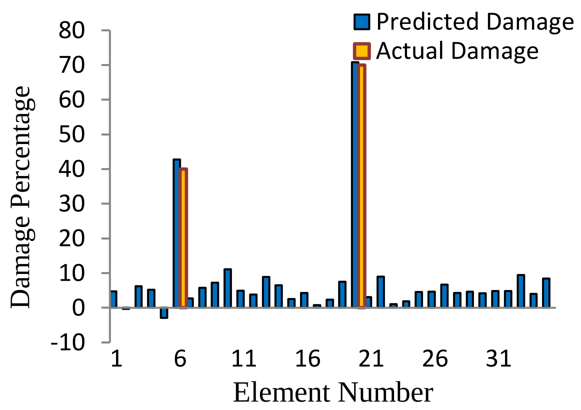

Fig. 18(a) The actual and predicted damage for the sixth damage scenarios considering 0.5% natural frequencies error

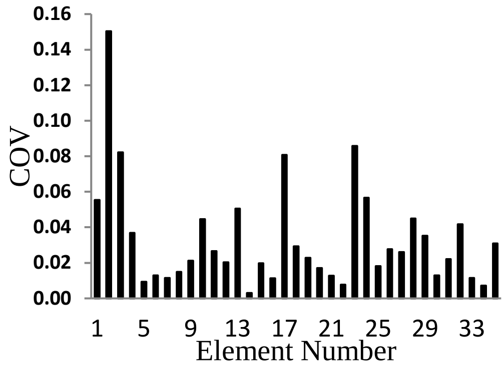

Fig. 18(b) COVs of estimated parameters for sixth damage scenarios considering 0.5% natural frequencies error

Table 5 Comparison of indices for model updating results considering 5% mass modeling error

Damage Scenarios		CI
1	measurement errors and mass modeling error	0.9017
	measurement errors and **without** mass modeling error	0.9635
4	measurement errors and mass modeling error	0.94
	measurement errors and **without** mass modeling error	0.9686

errors.

In order to gain a better evaluation of the accuracy of results, the closeness index (CI) is defined as (Bakhtiari Nejad *et al.* 2005)

$$\mathrm{CI} = 1 - \frac{|\delta \mathrm{P_P} - \delta \mathrm{P_t}|}{|\delta \mathrm{P_t}|} \tag{27}$$

Where, $\delta \mathrm{P_t}$ is the vector of true damage ratios and $\delta \mathrm{P_P}$ is the vector of the estimated damage parameters. For an accurate parameter estimation result, CI is close to one. The CI indices for model updating results considering natural frequencies error are given by Table 4. Comparison of the calculated CI indices by the corresponding indices using noise free natural frequencies prove that adverse effects of the natural frequency errors can be alleviated by appropriate selection of the excitation frequencies. In these cases, 10 percent of measurement errors are added to the PSD data.

Although in most real cases, the mass matrices of the structures are not changed by damage, there may also be some discrepancies between the real and assumed mass parameters used in the FE model of the structure. To consider this probable error, 5% of uniformly distributed random errors are added to the mass parameters of the elements. This modeling error can affect the eigenvectors of the intact structure which is used to construct the sensitivity equation of PSD. The results of the damage detecting process of two damage cases (1 and 4) considering inaccurate mass matrices are presented in Figs. 19 and 20. The damaged indices are given by Table 5. Low values of COVs of the estimated parameters proves that, by considering 5 percent random error in mass parameters, the parameter estimation process is still robust.

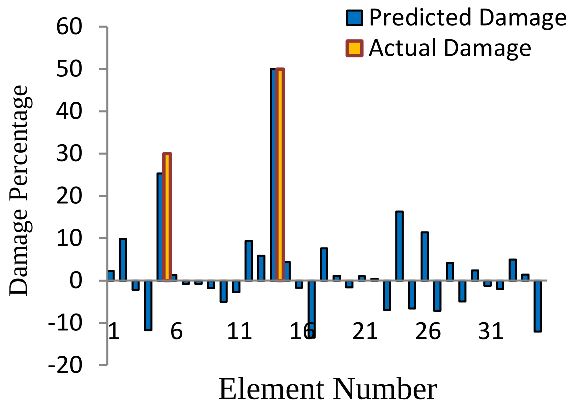

Fig. 19(a) The actual and predicted damage for first damage scenarios considering 5% mass modeling error

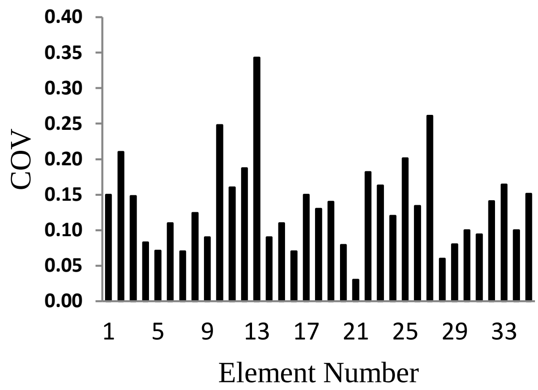

Fig. 19(b) COVs of the estimated parameters for first damage scenarios considering 5% mass modeling error

Table 6 CI indices for model updating results considering 15% measurement errors

Damage Scenarios		CI
2	15% measurement errors	0.95
	10% measurement errors	0.97
6	15% measurement errors	0.93
	10% measurement errors	0.94

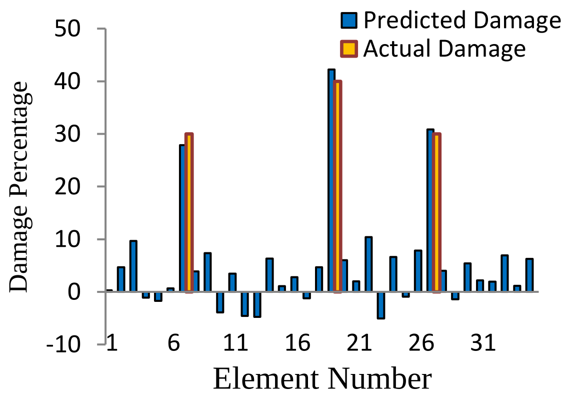

Fig. 20(a) The actual and predicted damage for fourth damage scenarios considering 5% mass modeling error

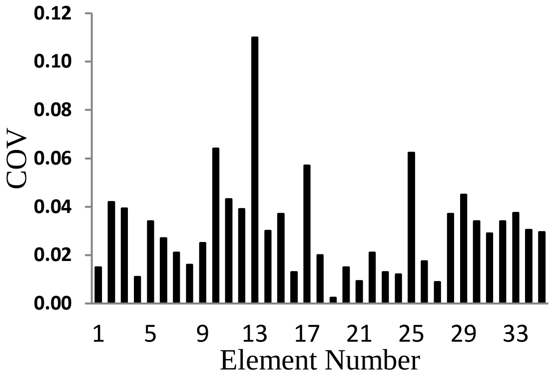

Fig. 20(b) COVs of the estimated parameters for fourth damage scenarios considering 5% mass modeling error

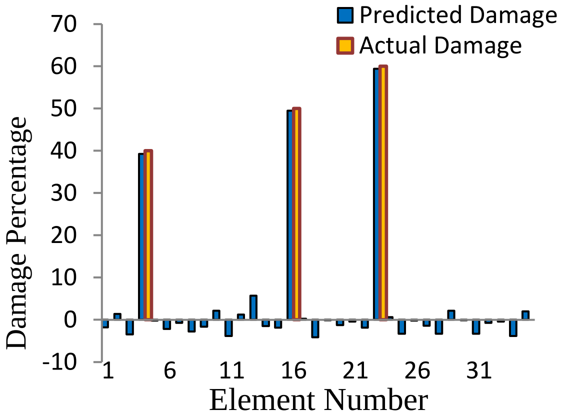

Fig. 21(a) The actual and predicted damage of second damage scenarios considering 15% measurement errors

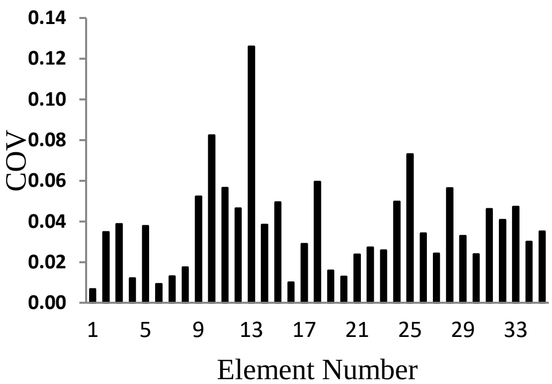

Fig. 21(b) COVs of the estimated parameters for the second damage scenario considering 15% measurement errors

For further investigation of the robustness of the proposed method against noise polluted data, noise level is increased to 15% for scenarios 2 and 6 and the corresponding parameter estimation results are shown in Figs. 21 and 22. The CI values are given by Table 6. Comparison of the results shows low effects of this level of the measurement errors on the model updating results.

In order to assess the performance of the proposed

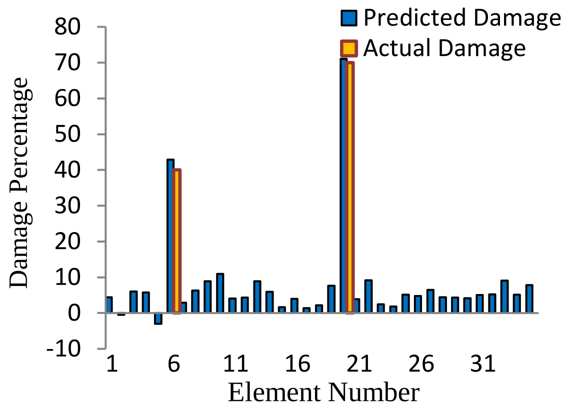

Fig. 22(a) The actual and predicted damage of sixth damage scenarios considering 15% measurement errors

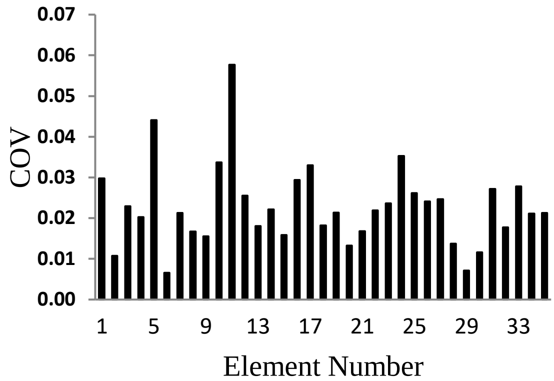

Fig. 22(b) COVs of the estimated parameters for the sixth damage scenario considering 15% measurement errors

Table 5 Comparison of indices for model updating results considering 5% mass modeling error

Damage Scenarios		CI
2	measurement errors	0.97
	measurement errors, natural frequency errors and mass modeling error	0.67
6	measurement errors	0.94
	measurement errors, natural frequency errors and mass modeling error	0.69

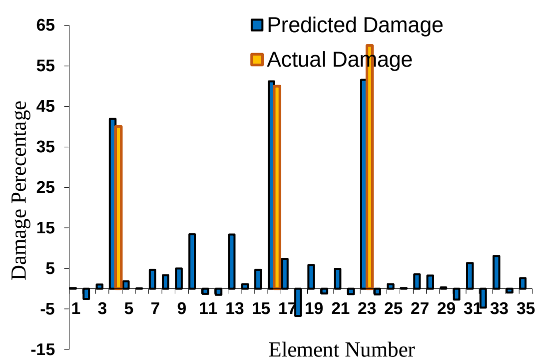

Fig. 23(a) The actual and predicted damage of second damage case considering mass modeling and natural frequencies errors

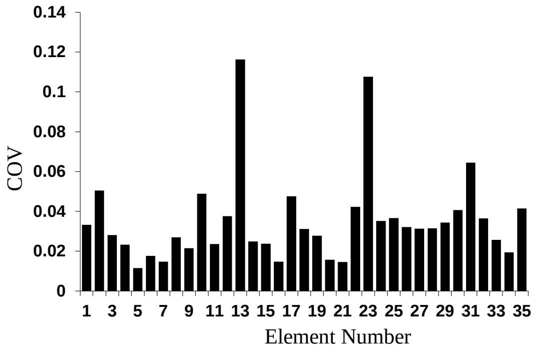

Fig. 23(b) COVs of the estimated parameters for the second damage case considering mass modeling and natural frequencies errors

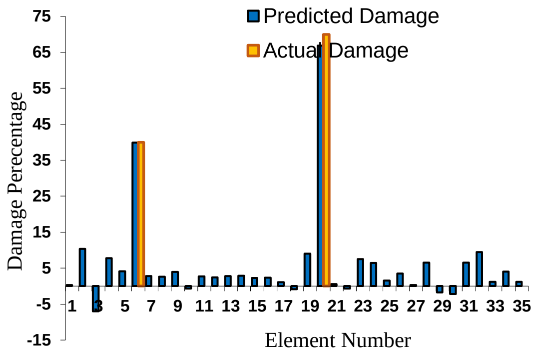

Fig. 24(a) The actual and predicted damage of sixth damage case considering mass modeling and natural frequencies errors

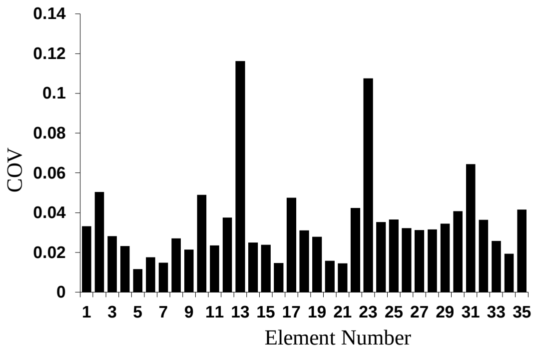

Fig. 24(b) COVs of the estimated parameters for the sixth damage case considering mass modeling and natural frequencies errors

model updating algorithm in more realistic cases, mass modelling errors and natural frequency errors are considered simultaneously. The parameter estimation results are plotted in Figs. 23 and 24. The CI values of the results are given by Table 7. The model updating results indicate that the proposed method is still robust in these cases.

As it was stated earlier the PSD is more sensitive to change of structural parameters in compare with the FRF. Hence, it is expected to be capable of more accurate parameter estimation especially for cases of low severity damage or highly noise contaminated data. In such cases change of structural response is low and might be

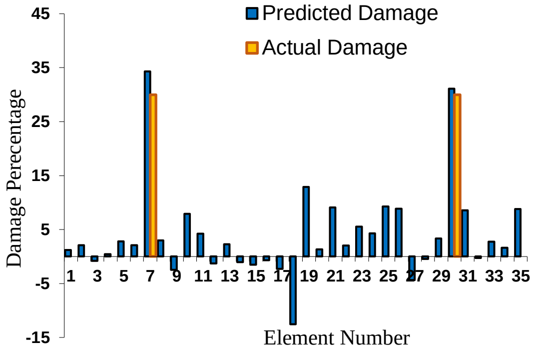

Fig. 25(a) The actual and predicted damage for first comparison scenarios by FRF Data

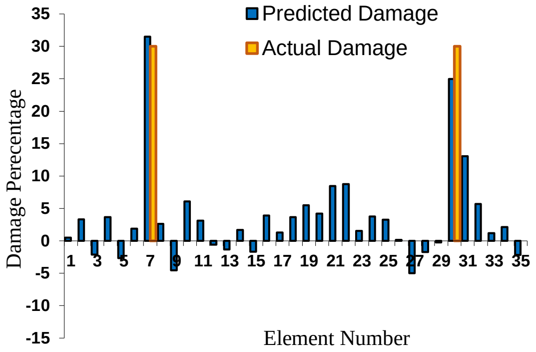

Fig. 25(b) The actual and predicted damage for first comparison scenarios by PSD Data

Table 7 Comparison of Closeness Index for the model updating results by FRF and PSD data

Damage Scenarios	CI	
	FRF-Based Method	PSD-Based Method
1	0.267	0.403
2	0.111	0.226
3	0.501	0.592
4	0.262	0.511

overshadowed by measurement errors. Also, model updating using excitation frequency of low ranges is a challenging issue, since change of structural responses is not significant and might be covered by unexpected measurement errors. For comparison of the performance of the proposed method based on PSD with a method based on FRF, several case of low severity damage is considered. The FRF sensitivity with respect to unknowns is estimated using a decomposed form of transfer function (Esfandiari *et al.* 2010). In this comparison study, excitation frequency ranges are considered the first four lower natural frequencies. The results of both PSD and FRF based model updating are presented considering 15% errors in simulated response of damaged structure. Comparison of the results presented in Figs. 25 to 28 proves the efficiency and robustness of model updating results using PSD data over the obtained results using FRF data, when working in lower frequency ranges.

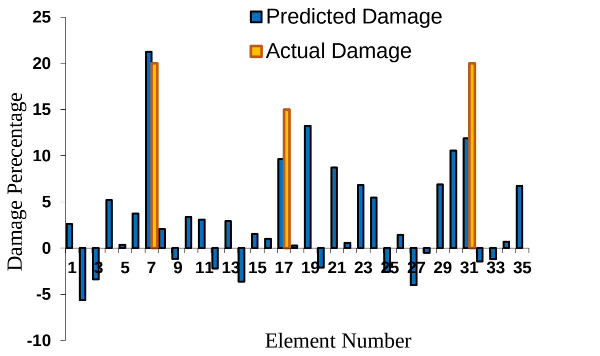

Fig. 26(a) The actual and predicted damage for second comparison scenarios by FRF Data

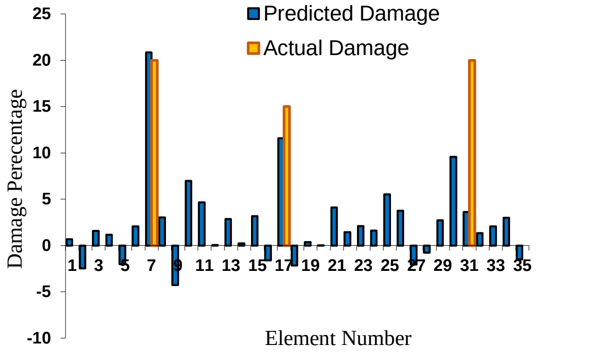

Fig. 26(b) The actual and predicted damage for second comparison scenarios by PSD Data

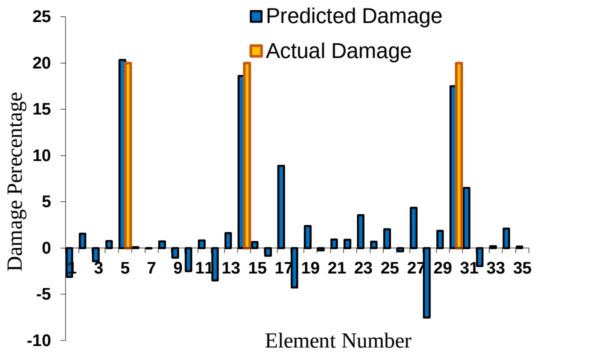

Fig. 27(a) The actual and predicted damage for third comparison scenarios by FRF Data

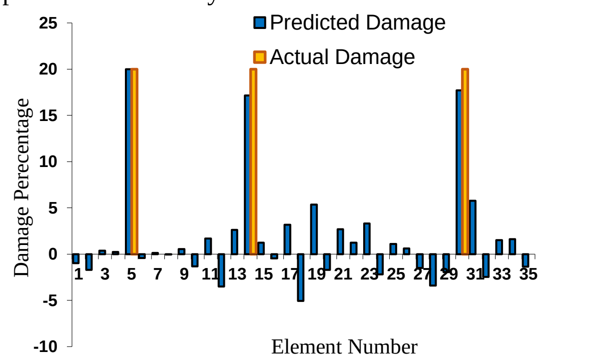

Fig. 27(b) The actual and predicted damage for third comparison scenarios by PSD Data

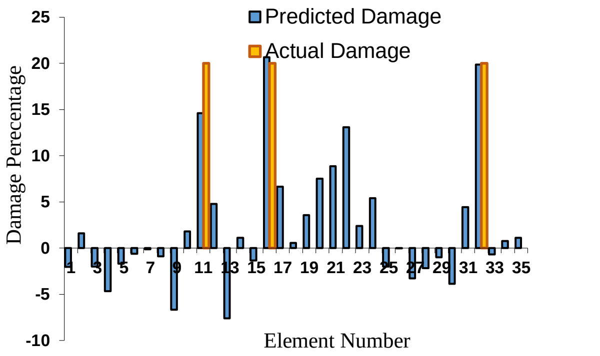

Fig. 28(a) The actual and predicted damage for fourth comparison scenarios by FRF Data

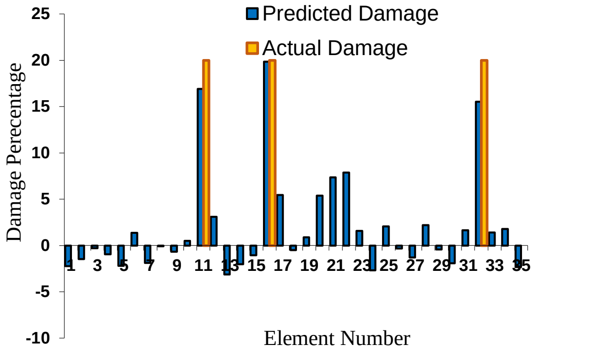

Fig. 29(b) The actual and predicted damage for fourth comparison scenarios by PSD Data

The quantitative comparison of the accuracy of the predicted structural parameters by both methods is conducted based on CI values of the results as given in Table 7. The results prove more accurate results by PSD based method.

In summary, this study showed that the proposed formulation for correlation of the PSD and changes of structural parameters yields a robust model updating method even in presence of high levels of noise. The results of this study also show that by appropriate selecting of the excitation frequency adverse effects of the natural frequency errors are alleviated. Furthermore, the results prove that the PSD are more sensitive to the changes of the structural parameters rather than FRF data.

4. Conclusions

A structural damage detection method is presented using the power spectral density function and partially measured natural frequencies of the damaged structure. The damage is considered as the change of the stiffness parameters. The change of the power spectral density function is expressed in terms of the changes of the mode shapes. The sensitivity equations are established through correlating the change of the power spectral density function of the structure to damage in elements. Sensitivity equations are solved by the least square method to compute the changes of structural parameters. The obtained numerical results of a truss model show the ability of the proposed method to identify location and severity of parameter changes at the elemental level in a structure. The results prove abilities of the method for model updating using highly noise contaminated data of low frequency ranges.

References

Araujo dos Santos, J.V., Mota Soares, C.M., Mota Soares, M.A. and Maia, N.M.M. (2005), "Structural damage identification in laminated structures using FRF data", *Compos. Struct.*, **67**(2), 239-249.

Bakhtiari Nejad, F., Rahai, A. and Esfandiari, A. (2004), "A structural damage detection method using static noisy data", *Eng. Struct.*, **27**(12), 1784-1793.

Bruggi, M. and Mariani, S. (2013), "Optimization of sensor placement to detect damage in flexible plates", *Eng. Optim.*, **45**(6), 659-676.

Ditommaso, R., Mucciarelli, M. and Ponzo F.C. (2012), "Analysis of non-stationary structural systems by using a band-variable filter", *Bull Earthq. Eng.*, **10**, 895-911.

Ditommaso, R. and Ponzo, F.C. (2015), "Automatic evaluation of the fundamental frequency variations and related damping factor of reinforced concrete framed structures using the short time impulse response function (STIRF)", *Eng. Struct.*, **82**, 104-112.

Ditommaso, R., Ponzo, F.C. and Auletta, G. (2015), "Damage detection on framed structures: modal curvature evaluation using Stockwell Transform under seismic excitation", *Earthq. Eng. Eng. Vibr.*, **14**(2), 265-274.

Entezami, A., Shariatmadar, H. and Sarmadi, H. (2017), "Structural damage detection by a new iterative regularization method and an improved sensitivity function", *J. Sound Vibr.*, **399**, 285-307.

Esfandiari, A., Bakhtiari-Nejad, F., Rahai, A. and Sanayei, M. (2009), "Structural model updating using frequency response function and quasi-linear sensitivity equation", *J. Sound Vibr.*, **236**(3), 557-573.

Esfandiari, A., Bakhtiari-Nejad, F., Sanayei, M. and Rahai, A. (2010), "Structural finite element model updating using transfer function data", *Comput. Struct.*, **88**(1-2), 54-64.

Eun, H.C., Cho, D.H., Ahn, Y.J. and Lee, S.G. (2015), "Damage identification of truss structure using power spectral density estimation", *Adv. Sci. Technol. Lett.*, **100**, 61-66.

Fan, W. and Qiao, P. (2011), "Vibration-based damage identification methods: A review and comparative study", *Struct. Health Monitor.*, **10**(1), 83-111.

Fox, R.L. and Kapoor, M.P. (1969), "Rates of change of eigenvalues and eigenvectors", *AIAA J.*, **6**(12), 2426-2429.

Gang, X., Chai, S., Allemang, R.J. and Li, L. (2014), "A new iterative model updating method using incomplete frequency response function data", *J. Sound Vibr.*, **333**, 2443-2453.

Kammer, D.C. and Nimityongskul, S. (2009), "Frequency band averaging of spectral densities for updating finite element models", *J. Vibr. Acoust.*, **131**(4), 041007-10.

Kim, B.H., Joo, H.J. and Park, T. (2007), "Damage evaluation of an axially loaded beam using modal flexibility", *KSCE J. Civil Eng.*, **11**(2), 101-110.

Kumar, R.P., Oshima, T., Mikami, S., Miyamori, Y. and Yamazaki, T. (2012), "Damage identification in a lightly reinforced concrete beam based on changes in the power spectral density", *Struct. Infrastruct. Eng.*, **8**(8), 715-727.

Li, Y.Y. and Chen, Y. (2013), "A review on recent development of vibration-based structural robust damage detection", *Struct. Eng. Mech.*, **45**(2), 159-168.

Li, J., Hao, H. and Lo, J.V. (2015), "Structural damage identification with power spectral density transmissibility: Numerical and experimental studies", *Smart Struct. Syst.*, **15**(1), 15-40.

Li, J., Hao, H., Xia, Y. and Zhu, H.P. (2015), "Damage assessment of shear connectors with vibration measurements and power spectral density transmissibility", *Struct. Eng. Mech.*, **54**(2), 257-289.

Liberatore, S. and Carman, G.P. (2004), "Power spectral density analysis for damage identification and location", *J. Sound Vibr.*, **274**, 761-776.

Liberatore, S., Carman, G.P. and Speyer, J.L. (2001), "Power spectral density (PSD) technique in damage detection", *Proceedings of the Spie-the International Society for Optical Engineering*., **4327**, 213-222.

Min, C.H., Hong, S., Park, S.Y. and Park, D.C. (2014), "Sensitivity-based finite element model updating with natural frequencies and zero frequencies for damped beam structures", *Int. J. Nav. Arch. Ocean*, **6**(4), 904-921.

Moradipour, P., Chan, T.H.T. and Gallage, C. (2015), "An improved modal strain energy method for structural damage detection, 2D simulation", *Struct. Eng. Mech.*, **54**(1), 105-119.

Natke, H.G., Lallement, G., Cottin, N. and Prells, U. (1995), "Properties of various residuals within updating of mathematical models", *Inv. Probl. Sci. Eng.*,**1**(4), 329-348.

Newland, D.E. (1993), *An Introduction to Random Vibration, Spectral and Wavelate Analysis*, 3rd Edition, John Wiley & Sons.

Pedram, M., Esfandiari, A. and Khedmati, M.R. (2017), "Damage detection by a FE model updating method using power spectral density: Numerical and experimental investigation", *J. Sound Vibr.*, **397**(9), 51-76.

Pedram, M., Esfandiari, A. and Khedmati, M.R. (2016), "Finite element model updating using strain-based power spectral density for damage detection", *Struct. Contr. Health Monitor.*, **23**, 1-15.

Petrovic, B., Parolai, S., Pianese, G., Dikmen, S.U., Moldobekov, B., Orunbaev, S. and Paolucci, R. (2017), "Joint deconvolution of building and downhole seismic recordings: An application to three test cases", *Bull Earthq. Eng*.

Sanayei, M. and Onipede, O. (1991) "Damage assessment of structures using static test data", *AIAA J.*, **29**(7), 1174-1179.

Wang, S.Q. and Li, H.J. (2012), "Assessment of structural damage using natural frequency changes", *Acta Mech. Sin.*, **28**(1), 118-127.

Xu, Y. and Zhu, W. (2017), "Non-model-based damage identification of plates using measured mode shapes", *Struct. Health Monitor.*, **16**(1), 3-23.

Yang, T. Fan, S.H. and Lin, C.H. (2003), "Joint stiffness identification using FRF measurements", *Comput. Struct.*, **81**, 2549-2556.

Yazdanpanah, O., Seyedpoor, S.M. and Akbarzadeh Bengar, H. (2015), "A new damage detection indicator for beams based on mode shape data", *Struct. Eng. Mech.*, **53**(4), 725-744.

Zhang, J., Xu, J.C., Guo, S.L. and Wu, Z.S. (2013), "Flexibility-based structural damage detection with unknown mass for IASC-ASCE benchmark studies", *Eng. Struct.*, **48**, 486-496.

Zheng, Z.D., Lu, Z.R., Chen, W.H. and Liu, J.K. (2015), "Structural damage identification based on power spectral density sensitivity analysis of dynamic responses", *Comput. Struct.*, **146**, 176-184.

CC